Research Article

Discrimination of six flathead fishes (Family: Platycephalidae) based on otolith morphology and morphometric features

Pathak V.[1]; Kumari G.[2]; Kumar Sharma S.[3]; Bhushan S.[1]; Jaiswar A.K.[1*]

Abstract

A taxonomic study on *Kumococius rodericensis* (Cuvier, 1829), *Grammoplites suppositus* (Troschel, 1840), *G. scaber* (Linnaeus, 1758), *Sorsogona tuberculata* (Cuvier, 1829), *Platycephalus indicus* (Linnaeus, 1758) and *Cociella crocodilus* (Cuvier, 1829) (family Platycephalidae) commonly occurring along the coast of India, was conducted to identify the traits which can easily differentiate the species. The study was based on samples (n=203) collected from landing centers of maritime states situated along the East and West coast of India from August 2015 to April 2016. In shape analysis no significant difference was observed at 95% level of confidence ($p<0.05$) between Left and right otolith and between male and female, so only the left otolith of all specimens considered for analysis for all species. The otolith of *S. tuberculata* was most rounded by 1.79 score among other species while otolith of *C. crocodilus* was more flat by 2.55 score. *K. rodericensis* and *G. scaber* had roundness score of more than 2.20 while *G. suppositus* and *P. indicus* had roundness scores less than 2.20. All species showed values of number of end points (points at the end of one pixel thick open branches) were zero except *C. crocodilus* that had a number of end points equal to 5, which showed that the periphery of otolith had five grooves larger than 1 pixel. The study disclosed a specific morphological and morphometric based characters of otolith that can be used to adjudicate the ambiguity in the flathead species.

Keywords: Groove, Morphometric, Otolith, Otolith periphery, Aragonite

1- ICAR – Central Institute of Fisheries Education, Versova, Mumbai – 400061, India
2- ICAR – Directorate of Coldwater Fisheries Research, Bhimtal – 263136, India
3- ICAR – Central Inland Fisheries Research Institute - Kolkata, West Bengal – 700120, India
*Corresponding author's Email: akjaiswarr@yahoo.com

Introduction

Otolith is a small stony structure mainly made up of calcium carbonate ($CaCO_3$), mostly in the form of aragonite located in the inner ear cavity of a teleost fish (Yedier and Bostancı, 2020). They grow continuously according to an accretionary process and the accretionary deposit is influenced both by environmental conditions and physiological parameters (Yedier *et al.*, 2018). This structure acts as a balancing and hearing organ (Campana, 1999; Campana and Thorrold, 2001). Otolith has a three-dimensional structure but it does not grow at the same rate in all dimensions (Campana and Thorrold, 2001); growth of otolith follows an allometric increase in dimensions (Chilton and Beamish, 1982). Also, shape and size vary considerably among species (Campana and Thorrold, 2001). 10% of otolith contain minor and trace elements within the aragonite matrix of otolith that are derived from the surrounding water of fish habitat. These impurities show water chemistry and fish's metabolism (Campana and Thorrold, 2001; Telmer, 2004).

Morphological characteristics of fish otoliths are highly variable among species, ranging from a simple disc shape in some flatfish (Pleuronectidae) to an irregular shape in other fish species such as redfish, *Sebastes* sp. (Hunt, 1992).

Otolith plays a vital role in fisheries research during 21st century. It plays a diverse role in research areas like annual age and growth, otolith microstructure, hearing and balance, population dynamics, otolith allometry, species identification, tracer application, mass marking, trace element, environmental reconstruction, isotopes, fossils record, physiology, otolith chemistry, larval fish ecology, etc. Some thrusted and challenging research areas related to otolith are otolith growth model, chemical tracer, relationship between otolith, weight and age, etc. (Campana, 2005; Xu, 2014; Fisher and Hunter, 2018; Thomas and Swearer, 2019).

Materials and methods

A total of 203 fish specimens belonging to six species, namely *K. rodericensis* (37), *G. suppositus* (30), *S. tuberculate* (39), *P. indicus* (21), *G. scaber* (40), *C. crocodilus* (36) were collected from trawl landings in Porbandar, Veraval (Gujarat), Sassoondock , Newferry wharf, Versova (Mumbai, Maharashtra) on West coast, and Mandapam, Kilakarai (Tamilnadu), Digha (West Bengal) on East coast of India during August 2015 to April 2016 (Fig. 1). Fishes were identified up to species level by using the available keys in FAO species identification sheets (FAO, 1984). Sagittal otoliths were collected from freshly collected fish samples by dissecting from the ventral surface.

The collected otoliths were cleaned using distilled water, dried, photographed dorsally, and stored in airtight vials. The outline of associated features (Fig. 2) was used to compare differences across species and genera. The terminology used for otoliths description was followed as described

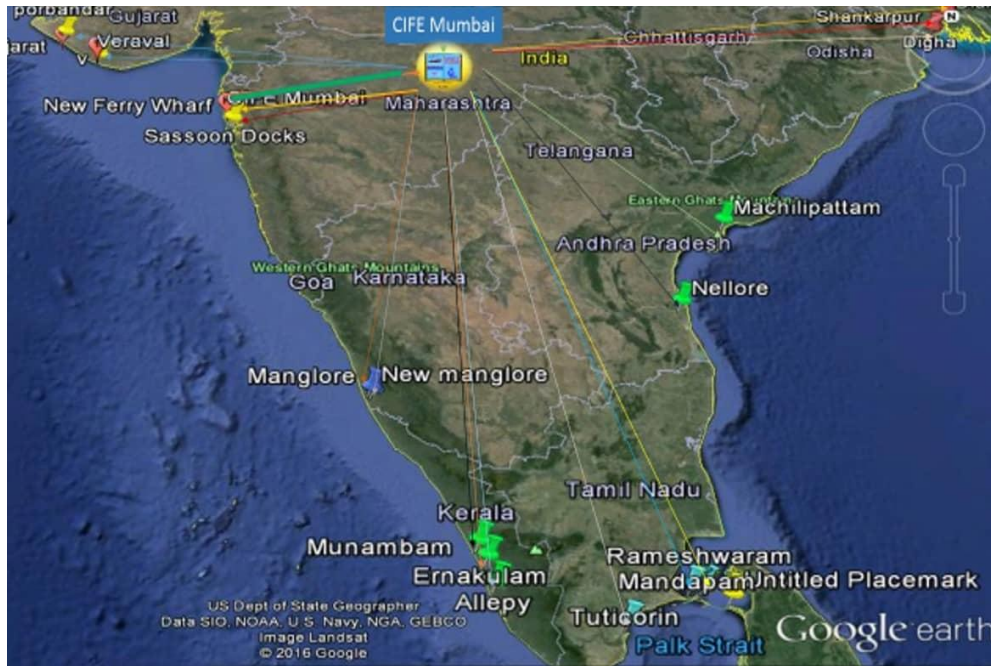by Tuset *et al.*, 2008 and Bostanci *et al.*, 2015.
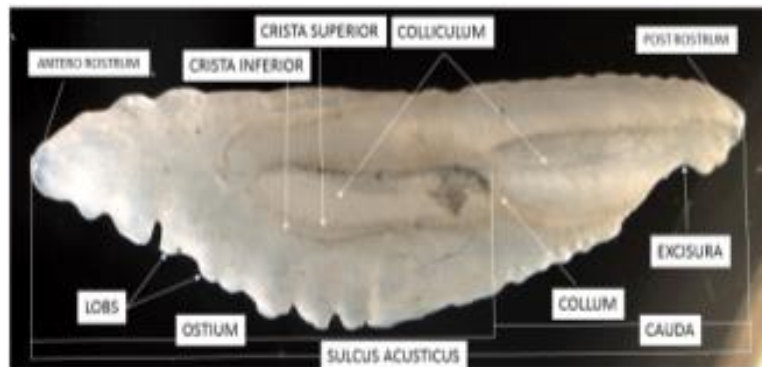

Figure 1: Sampling sites throughout Indian water.

Figure 2: General morphological features of Otolith for species identification.

Incremental distance analysis

Incremental distance analysis works by finding and maintaining the pair of closest features (vertex, edge, or face) on the two polyhedral. The advantage is that the closest features change only infrequently as the objects move along finely discretized paths. By preprocessing the polyhedral, it can verify that the closest features have not changed in constant time. The experiments showed that, once initialized, the algorithm's expected running time is constant, independent of the complexity of the polyhedral (Lin and Canny, 1991).

The algorithm is that, to compute distances and closest points from there, it can easily compute gradients of the distance function in configuration space, thereby finding the direction of the maximal

clearance curves.

Results

In the analysis, no significant difference was observed at 95% confidence (*p*<0.05) between left and right otoliths and between male and female fish specimens so only left otolith of all specimens considered for analysis of all species.

Kumococius rodericensis (Cuvier, 1829), spiny flathead: Otolith was elongated, anterior and posterior ends of otolith (rostrum) were pointed and slightly curved towards dorsal side, both dorsal and ventral margins lacked serration. Mid to anterior part was narrower than mid to posterior part.

The ostium and cauda were bi-lobed and nearly of the same length, colliculum was not clearly visible, crista superior and crista inferior also were not clearly visible (Fig. 3).
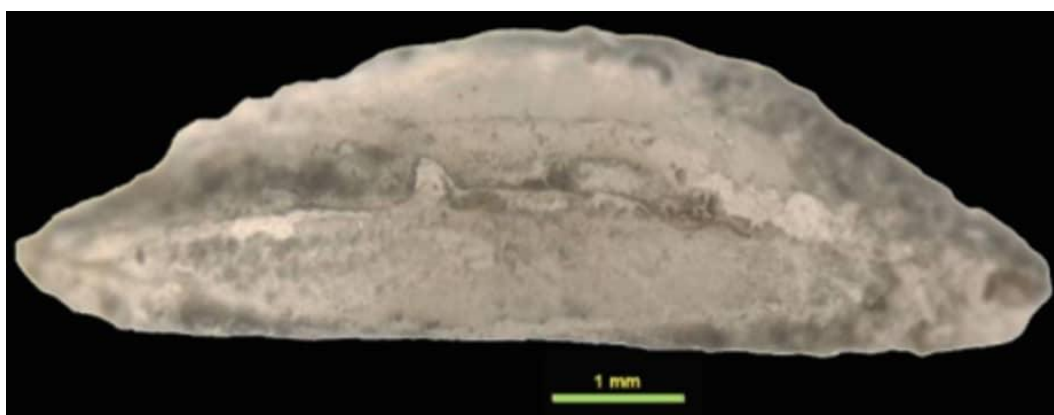

Figure 3: Left otolith of *Kumococius rodericensis*.

Mean ferret diameter (caliper length) along minor axis of region was 590.72 pixels. Measure of roundness [(perimeter^2)/4 pi. area)] of otolith showed elliptical shape of otolith with a value of 2.21. The radius (distance between region centroid and boundary) of otolith varied between 227.65 to 1151.25 pixels; hence, the ratio of radii was 5.06. The perimeter bounding (chain code length of the outline) of otolith was 5097.21 pixels. Number of end points (points at the end of one pixel thick open branches) was zero, i.e. no creation on periphery of otolith (Table 1).

Grammoplites suppositus (Troschel, 1840), spotfin flathead: The antero rostral end of otolith was narrower than posterior with smooth anterior end while post rostrum was blindly smooth rounded. Ventral part of otolith was straight and dorsal part was convex, there was no serration on periphery.

Colliculum had a single lobe, and was widely open on periphery, posterior part of colliculum had tube like structure, crista inferior and crista superior were not distinct and collum was not visible (Fig. 4).

Table 1: Comparative statistical analysis of otolith of all species.

Spp	No.	Width(pix)	Roundness	Radius, Min(pix)	Radius, Max(pix)	Radius Ratio	Perimeter, Bounding Pixels(pix)	Number of End Points
K. rodericensis	37	590.72	2.21	227.65	1151.25	5.06	5097.21	0
G. suppositus	30	624.85	2.01	263.21	1049.06	3.99	4629.49	0
S. tuberculate	39	727.87	1.79	306.28	1029.55	3.36	4816.95	0
P. indicus	21	662.63	1.87	306.24	1004.28	3.28	4605.37	0
G. scaber	40	519.86	2.49	204.95	1160.22	5.66	5007.81	0
C. crocodilus	36	894.55	2.55	331.87	1159.31	3.49	6442.04	5

Figure 4: Left otolith of *Grammoplites suppositus*.

Mean ferret diameter (caliper length) along minor axis of region was 624.85 pixels. Measure of roundness [(perimeter^2)/4 pi. area)] of otolith showed elliptical shape of otolith with a value of 2.01. The radius (distance between region centroid and boundary) of otolith varied between 263.21 to 1049.06 pixels; the ratio of radii was 3.99. The perimeter bounding (chain code length of the outline) of otolith was 4629.49 pixels. Number of end points (points at the end of one pixel thick open branches) was zero, i.e. no creation on periphery of otolith (Table 1).

Sorsogona tuberculata (Cuvier, 1829), tuberculated flathead: Ventral part of otolith was straight to convex while dorsal part was convex in shape. Antero rostrum was blunt in shape and post rostrum was narrower than mid part of otolith, there was no serration on periphery.

There was a single lobe, equidistance Crista inferior, crista superior and collum were not distinct (Fig. 5).
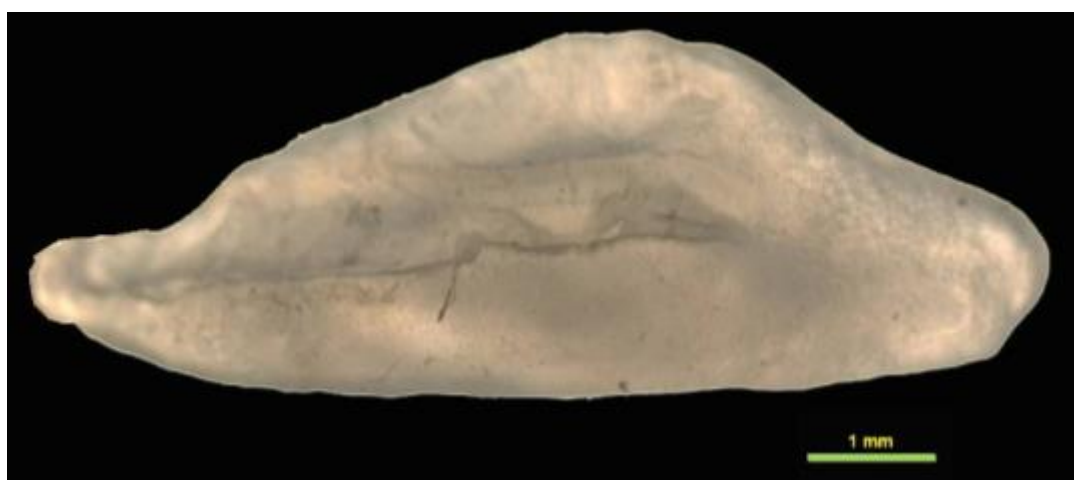
Figure 5: Left otolith of *Sorsogona tuberculata*.

Mean ferret diameter (caliper length) along minor axis of region was 727.87 pixels. Measure of roundness [(perimeter^2)/4 pi. area)] of otolith showed elliptical shape of otolith with a value of 1.79. The radius (distance between region centroid and boundary) of otolith varied between 306.28 to 1029.55 pixels; the ratio of radii was 3.36. The perimeter bounding (chain code length of the outline) of otolith was 4816.95 pixels. Number of end points (points at the end of one pixel thick open branches) was zero, i.e. no creation on periphery of otolith (Table 1).

Platycephalus indicus (Linnaeus, 1758), bartail flathead: Otolith was bi-lobed, anterior lobe was much larger than the posterior lobe, anterior rostrum was pointed and slightly curved in upward direction, and post rostrum in second lobe was blunt in shape. Both dorsal and ventral parts were straight to convex in shape.

Colliculum was without collum. Mid part of the otolith had two flat canals like strip and excisura major in between both lobes present. There was no serration on periphery. Cauda and ostium were unseparated; sulcus cover was more than 2/3 part of otolith (Fig. 6).

Mean ferret diameter (caliper length) along minor axis of region was 662.63 pixels. Measure of roundness [(perimeter^2)/4 pi. area)] of otolith showed elliptical shape of otolith with a value of 1.87. The radius (distance between region centroid and boundary) of otolith varied between 306.24 to 1004.28 pixels; the ratio of radii was 3.28. The perimeter bounding (chain code length of the outline) of otolith was 4605.37 pixels. Number of end points (points at the end of one pixel thick open branches) was zero, i.e. no creation on periphery of otolith (Table 1).

Grammoplites scaber (Linnaeus, 1758), rough flathead: Otolith was elongated with pointed anterior rostrum, excisura minor was present, posterior rostrum was also pointed without excisura major. Ventral periphery was straight while dorsal margin was convex in shape.

Many pits were visible on the mid part of the otolith.

Figure 6: Left otolith of *Platycephalus indicus*.

Cauda and ostium were visible in a side by side arrangement. Ostium was smaller than cauda with accessory pits. Crista superior and sulcus acusticus were clearly seen (Fig. 7).
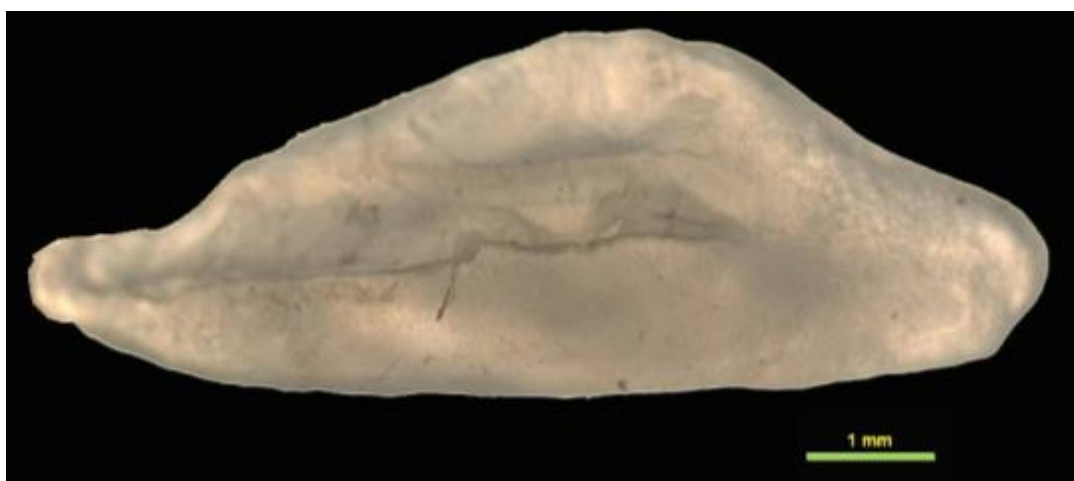
Figure 7: Left otolith of *Grammoplites scaber*.

Mean ferret diameter (caliper length) along minor axis of region was 519.86 pixels. Measure of roundness [(perimeter^2)/4 pi. area)] of otolith showed elliptical shape of otolith with a value of 2.49. The radius (distance between region centroid and boundary) of otolith varied between 204.95 to 1160.22 pixels; the ratio of radii was 5.66. The perimeter bounding (chain code length of the outline) of otolith was 5007.81 pixels. Number of end points (points at the end of one pixel thick open branches) was zero, i.e. no creation on periphery of otolith (Table 1).

Cociella crocodilus (Cuvier, 1829), crocodile flathead: Otolith had rough periphery with small spine like

structures on ventral margin and finely serrated lobe on the dorsal side of the otolith. The rostrum was posteriorly narrow and was broader anteriorly. Excisura minor and excisura major were both present.

Single lobed colliculum with exterior opening was clearly visible. Crista superior was zig zag in shape, ostium and cauda were fused, and collum was not visible (Fig. 8).

Figure 8: Left otolith of *Cociella crocodilus*.

Mean ferret diameter (caliper length) along minor axis of region was 845.55 pixels. Measure of roundness [(perimeter^2)/4 pi. area)] of otolith showed elliptical shape of otolith with a value of 2.55. The radius (distance between region centroid and boundary) of otolith varied between 331.87 to 1159.31 pixels; ratio of radii was 3.49. The perimeter bounding (chain code length of the outline) of otolith was 6442.04 pixels. Number of end points (points at the end of one pixel thick open branches) was 5, i.e. many creations on periphery of the otolith (Table 1).

Comparative statistical analysis of otoliths of all species
The otolith of *S. tuberculata* was the most rounded by 1.79 score among other species, while otolith of *C. crocodilus* was more flat by 2.55 score. *K.*

rodericensis and *G. scaber* had roundness scores more than 2.20, while *G. suppositus* and *P. indicus* had roundness scores less than 2.20. The percentage ratio (largest radii/smallest radii) was found to be maximum in *G. scaber* and minimum in *P. indicus. K. rodericensis* and *G. suppositus* had ratio values more than 3.50, while *S. tuberculata* and *C. crocodilus* had values less than 3.5. Perimeter, bounding was highest in case of *C. crocodilus* (6442.04 pixels) and lowest in *P. indicus* (4605.37 pixels). *K. rodericensis* and *G. scaber* showed perimeter, bounding values of more than 5000 pixels, while *G. suppositus* and *S. tuberculata* had value less than 5000 pixels. Values of number of end points of all species were zero except *C. crocodilus* that had a number of end points equal to 5, which showed that the

periphery of the otolith had five grooves larger than 1 pixel.

Morphology of otolith

The ostium and cauda of *K. rodericensis* both were bi-lobed and nearly of same length, colliculum was not clearly visible, crista superior and crista inferior also were not clearly visible. Colliculum of *G. suppositus* had a single lobe, and was widely open on periphery; posterior part of colliculum had tube like structure. The colliculum of *S. tuberculata* had a single lobe, had equidistance canal like present. Crista inferior, crista superior and collum were not distinct. Colliculum of *P. indicus* was without collum, on mid part of the otolith two flat canals like strips were present and excisura major-in between both lobes was present. There was no serration on periphery. Cauda and ostium were not separated; sulcus covered more than 2/3 part of the otolith. Cauda and ostium of *G. scaber* were visible in a side by side arrangement. Ostium was smaller than cauda with accessory pits. Crista superior and sulcus acusticus were clearly seen. And in *C. crocodilus* single lobed colliculum with exterior opening was clearly visible. Crista superior was zig zag in shape, ostium and cauda were fused, collum was not visible.

Discussion

This analysis is not done in any earlier study for description and identification of Platycephalidae. Work on otolith morphology for the genus *Serranus* is done by Flusser and Suk (1993), Voss

and Suesse (1997), Sonka *et al.* (1998), Bowman *et al.* (2001), Zunic and Rosin (2004), and Rosin (2005).

Environmental factors, such as water depth, salinity, topography, temperature are advised to be responsible for differences in otolith parameter such as otolith length, area (Lombarte *et al.*, 2010; Reichenbacher and Reichard, 2014). However, several morphometric parameters of otolith, such as otolith size, sulcus morphology and rostrum size are mostly under genetic influence or control in the same genera of fishes. Hence, the systematic importance of otoliths is well accepted (Gierl *et al.*, 2013).

The present study revealed no significant difference between left and right otoliths in all species as also reported in earlier works (Hunt, 1979; Harvey *et al.*, 2000; Waessle *et al.*, 2003). Most of the previous researchers focused on relationships between otolith parameters (length, weight, perimeter, width, area, roundness, circularity, ellipticity, rectangularity, aspect ratio) and fish size (total length and total weight) in different fish species (Harvey *et al.*, 2000; Waessle *et al.*, 2003; Battaglia *et al.*, 2010, 2015).

Hard parts, such as otoliths, are important tools for age determination (Kontaş *et al.*, 2020). Divergence of species is strongly correlated with divergence of otolith (Tuset *et al.*, 2020). Yedier *et al.* (2019) also discriminated fish species successfully based on otolith features, such as otolith width, sulcus shap, ostium, and cauda of the otolith.

Bostanci *et al.* (2015, 2016) and Yedier *et al.* (2016) investigated morphological and biometric characteristics as well as shape indices of both sides of sagittal otoliths and reported otolith as tools for species identification. Tuset *et al.* (2008) provided otolith atlas of 348 species of western Mediterranean Sea for species identification that support the present investigation.

The present investigation can be used as a helpful tool in predicting fish size from the otoliths and calculating the biomass of these less studied fish species during feeding studies. These data also help taxonomic discrimination of the species.

This study on otolith of fish family Platycephalidae discriminated species by otolith morphometric features. This analysis is not done in any earlier study for Platycephalidae fishes. The data of the study is helpful for knowing the type of habitat substratum, swimming pattern, resolving ambiguity with cryptic species, proper identification, age and growth analysis, variation in shape, etc.

Acknowledgments

Reference

Battaglia, P., Malara, D., Romeo, T. and Andaloro, F., 2010. Relationships between otolith size and fish size in some mesopelagic and bathypelagic species from the Mediterranean Sea (Strait of Messina, Italy). *Scientia Marina*, 74(**3**), 605–612. DOI:10.3989/scimar.2010.74n3605.

Battaglia, P., Malara, D., Ammendolia, G., Romeo, T. and Andaloro, F., 2015. Relationships between otolith size and fish length in some mesopelagic teleosts (Myctophidae, Paralepididae, Phosichthyidae and Stomiidae). *Journal of Fish Biology*, 87(**3**), 774–782. DOI:10.1111/jfb.12744.

Bostanci, D., Polat, N., Kurucu, G., Yedier, S., Kontaş, S. and Darçin, M., 2015. Using otolith shape and morphometry to identify four *Alburnus* species (*A. chalcoides*, *A. escherichii*, *A. mossulensis* and *A. tarichi*) in Turkish inland waters. *Journal of Applied Ichthyology*, 31(**6**), 1013–1022. DOI:10.1111/jai.12860.

Bostanci, D., Yilmaz, M., Yedier, S., Kurucu, G., Kontas, S., Darçin, M. and Polat, N., 2016. Sagittal otolith morphology of sharpsnout seabream *Diplodus puntazzo* (Walbaum, 1792) in the Aegean Sea. *International Journal of Morphology*, 34(**2**), 484–488. DOI:10.4067/s0717-95022016000200012.

Bowman, E.T., Soga, K. and Drummond, W., 2001. Particle shape characterisation using Fourier descriptor analysis. *Géotechnique*, 51(**6**), 545–554. DOI:10.1680/geot.2001.51.6.545.

Campana, S.E. and Thorrold, S.R., 2001. Otoliths, increments, and elements: keys to a comprehensive understanding of fish populations?

Canadian Journal of Fisheries and Aquatic Sciences, 58(**1**), 30–38. DOI:10.1139/f00-177.

Campana, S.E., 1999. Chemistry and composition of fish otoliths: pathways, mechanisms and applications. *Marine Ecology Progress Series*, 188, 263–297. DOI:10.3354/meps.188263.

Campana, S.E., 2005. Otolith science entering the 21st century. *Marine and Freshwater Research*, 56(**5**), 485–495. DOI:10.1071/mf04147.

Chilton, D.E. and Beamish, R.J., 1982. Age determination methods for fishes studied by the groundfish program at the Pacific Biological Station. Canadian Special Publication of Fisheries and Aquatic Sciences, 60, 102 P. Department of Fisheries and Oceans, Resource Services, Pacific Biological Station, Nanalmo, British Columbia, Canada.

FAO, 1984. FAO species identification sheets for fishery purposes. FAO Fisheries Department, Rome, Italy.

Fisher, M. and Hunter, E., 2018. Digital imaging techniques in otolith data capture, analysis and interpretation. *Marine Ecology Progress Series*, 598, 213–231. DOI:10.3354/meps12531.

Flusser, J. and Suk, T., 1993. Pattern recognition by affine moment invariants. *Pattern Recognition*, 26(**1**), 167-174. DOI:10.1016/0031-3203(93)90098.h.

Gierl C., Reichenbacher B., Gaudant J., Erpenbeck D. and Pharisat A., 2013. An extraordinary gobioid fish fossil from southern France. *PLoS*

One, 8(**5**), e64117. DOI:10.1371/journal.pone.0064117.

Harvey, J.T., Loughlin, T.R., Perez, M.A. and Oxman, D.S., 2000. Relationship between fish size and otolith length for 63 species of fishes from the eastern North Pacific Ocean. NOAA technical report NMFS 150. A technical report of the Fishery Bulletin. US Department of Commerce, Seattle, Washington, USA. 36 P.

Hunt, J.J., 1979. *Back calculation of length at age from otoliths for silver hake of the Scotian Shelf, Canada.* Selected Paper No. 5, International Commission for the Northwest Atlantic Fishery, Dartmouth, Nova Scotia, Canada, 11–17.

Hunt, J.J., 1992. Morphological characteristics for otoliths of selected fish in the Northwest Atlantic. *Journal of Northwest Atlantic Fishery Science*, 13, 63–75. DOI:10.2960/j.v13.a5.

Kontaş, S., Yedier, S. and Bostancı, D., 2020. Otolith and scale morphology of endemic fish *Cyprinion macrostomum* in Tigris–Euphrates Basin. *Journal of Ichthyology*, 60(**4**), 562–569. DOI:10.1134/s0032945220040086.

Lin, M.C. and Canny, J.F. 1991. A fast algorithm for incremental distance calculation. Proceedings of the IEEE International Conference on Robotics and Automation, 9-11 April 1991, Sacramento, California, USA, 1008–1014. DOI:10.1109/robot.1991.131723.

Lombarte, A., Palmer, M., Matallanas, J., Gómez-Zurita, J. and Morales-Nin, B., 2010. Ecomorphological trends and phylogenetic inertia of otolith sagittae in Nototheniidae. *Environmental Biology of Fishes*, 89, 607–618. DOI:10.1007/s10641-010-9673-2.

Reichenbacher, B. and Reichard, M., 2014. Otoliths of five extant species of the annual killifish *Nothobranchius* from the East African savannah. *PLoS One*, 9(**11**), e112459. DOI:10.1371/journal.pone.0112459.

Rosin, P. L., 2005. *Computing global shape measures*. In: Handbook of pattern recognition and computer vision, 3rd edition. Chen, C.H. and Wang, P.S.P., editors. World Scientific Publishing Co., Singapore, 177–196. DOI:10.1142/9789812775320_0010.

Sonka, M., Hlavac, V. and Boyle, R., 1998. *Image processing, analysis, and machine vision*, 2nd edition. Cengage Learning, Boston, Massachusetts, USA, 800 P.

Telmer, K., 2004. Fish otoliths. http://web.uvi.ca/čktelmer/fishoto.html.

Thomas, O.R. and Swearer, S.E., 2019. Otolith biochemistry - a review. *Reviews in Fisheries Science and Aquaculture*, 27(**4**), 458–489. DOI:10.1080/23308249.2019.1627285.

Tuset, V.M., Lombarte, A. and Assis, C.A., 2008. Otolith atlas for the western Mediterranean, north and central eastern Atlantic. *Scientia Marina*, 72(**s1**), 7–198. DOI:10.3989/scimar.2008.72s17.

Tuset, V.M., Lombarte, A., Bariche, M., Maynou, F. and Azzurro, E., 2020. Otolith morphological divergences of successful Lessepsian fishes on the Mediterranean coastal waters. *Estuarine, Coastal and Shelf Science*, 236, 106631. DOI:10.1016/j.ecss.2020.106631.

Voss, K. and Suesse, H., 1997. Invariant fitting of planar objects by primitives. *IEEE Transactions on Pattern Analysis and Machine Intelligence*, 19(1), 80–84. DOI:10.1109/34.566815.

Waessle, J.A., Lasta, C.A. and Favero, M., 2003. Otolith morphology and body size relationships for juvenile Sciaenidae in the Río de la Plata estuary (35-36°S). *Scientia Marina*, 67(**2**), 233–240. DOI:10.3989/scimar.2003.67n2233.

Xu, Y., 2014. *Application of otolith increment analysis to the study of maturation timing in female kokanee salmon.* Master of Science Thesis, University of Western Ontario, London, Ontario, Canada. Electronic Thesis and Dissertation Repository, 2601.

Yedier, S., Kontaş, S., Bostancı, D. and Polat, N., 2016. Otolith and scale morphologies of doctor fish (*Garra rufa*) inhabiting Kangal Balıklı Çermik thermal spring (Sivas, Turkey). *Iranian Journal of Fisheries Sciences*, 15(**4**), 1593–1608.

Yedier, S., Bostanci, D., Kontaş, S., Kurucu, G. and Polat, N., 2018.

Comparison of otolith mass asymmetry in two different *Solea solea* populations in Mediterranean Sea. *Ordu University Journal of Science and Technology*, 8(**1**), 125–133.

Yedier, S., Bostanci, D., Kontaş, S., Kurucu, G., Apaydin Yağci, M. and Polat, N., 2019. Comparison of otolith morphology of invasive big-scale sand smelt (*Atherina boyeri*) from natural and artificial lakes in Turkey. *Iranian Journal of Fisheries Sciences*, 18(**4**), 635–645. DOI:10.22092/ijfs.2018.116980.

Yedier S. and Bostancı, D., 2020. Aberrant otoliths in four marine fishes from the Aegean Sea, Black Sea, and Sea of Marmara (Turkey). *Regional Studies in Marine Science*, 34, 101011. DOI:10.1016/j.rsma.2019.101011.

Zunic, J. and Rosin, P.L., 2004. A new convexity measure for polygons. *IEEE Transactions on Pattern Analysis and Machine Intelligence*, 26(**7**), 923–934. DOI:10.1109/tpami.2004.19.